

# Towards Assessing the Violence of Reaction During Cookoff of Confined Energetic Materials\*

M. R. Baer, M. E. Kipp, R. G. Schmitt, & M. L. Hobbs  
*Sandia National Laboratories*  
*Albuquerque, New Mexico 87185 USA*

## ABSTRACT

An analysis of post-ignition events in a variable confinement cookoff test<sup>1</sup> (VCCT) geometry is presented aimed toward predicting the level of violence during cookoff of confined thermally-degraded energetic materials. This study focuses on the dynamic events following thermal initiation whereby accelerated combustion interacts with confinement. Numerical simulations, based on a model of reactive multiphase mixtures, indicate that the response of energetic material is highly dependent upon thermal/mechanical damage states prior to ignition. These damaged states affect the rate of pressurization, dynamic compaction behavior and subsequent growth to detonation. Variations of the specific surface area and porosity produced by decomposition of the energetic material causes different responses ranging from pressure burst to detonation. Calculated stress histories are used in estimating breakup of the VCCT confinement based on Grady-Kipp fragmentation theory<sup>2</sup>.

## INTRODUCTION

# MASTER

Cookoff involves coupled thermal/chemical/mechanical processes that create thermal damage of the energetic material which favor conditions for self-accelerated combustion and enhance shock sensitivity. Predictive finite element-based analysis tools are being developed at Sandia National Laboratories<sup>3</sup> to assess the level of violence including the coupled effects of heat transfer with chemistry, quasi-static structural mechanics and dynamic response. Detailed modeling of cookoff, in its entirety, is not currently possible. Despite the years of study in cookoff phenomena, relatively little is known about thermally-degraded energetic materials. Recent work has suggested that thermal decomposition causes significant changes in microstructure in the energetic material forming regions of porosity with high specific surface area<sup>4</sup>.

During heatup in a cookoff event, thermal stresses and material decomposition cause a buildup of quasi-static stress in the confinement. Given sufficient heating, exothermic energy release can exceed that dissipated by thermal conduction, and self-sustained reaction is possible. Once ignition occurs, the response of the confined energetic material becomes dynamic and the level of violence is determined by the evolution of pressure as combustion sweeps through the thermally-damaged material. The competition between pressure buildup and stress release due to the loss of confinement determines the level of violence of the event. Thus, the outcome of the event greatly depends on the thermally-damaged states evolving prior to ignition.

Current research has been directed at determining appropriate combustion<sup>5</sup> and stress-strain data<sup>6</sup> for damaged energetic materials. Predictive cookoff modeling requires multidimensional multi-material analysis capable of resolving phenomena spanning twelve orders of magnitude in time, from ten's of hours to sub-microseconds. An ambitious effort at Lawrence Livermore National Laboratory is underway in developing ALE3D<sup>7</sup> as a single platform for cookoff modeling. At Sandia National Laboratories, a different modeling strategy is being taken. Existing analysis capabilities are coupled and applied to material characterization experiments to determine appropriate combustion physics models for cookoff. Then, finite element thermal and stress analysis are merged with shock physics analysis. In this work, the effects of dynamic combustion are studied that link quasi-static and dynamic combustion behavior. An overview of the finite element thermal and stress analysis is not repeated in this work; the interested reader can find such information in references 8 and 9.

In the sections to follow, a brief description of mixture theory and its implementation into the shock physics code is presented. Demonstrative numerical simulations of cookoff in the variable confinement cookoff test (VCCT) are then discussed which illustrate that various states of thermal damage (i.e. porosity and specific surface area) lead to different levels of violence and modes of combustion. Then, the breakup of confinement is estimated using Grady-

\*Approved for public release; distribution is unlimited

## **DISCLAIMER**

**Portions of this document may be illegible  
in electronic image products. Images are  
produced from the best available original  
document.**

## **DISCLAIMER**

This report was prepared as an account of work sponsored by an agency of the United States Government. Neither the United States Government nor any agency thereof, nor any of their employees, makes any warranty, express or implied, or assumes any legal liability or responsibility for the accuracy, completeness, or usefulness of any information, apparatus, product, or process disclosed, or represents that its use would not infringe privately owned rights. Reference herein to any specific commercial product, process, or service by trade name, trademark, manufacturer, or otherwise does not necessarily constitute or imply its endorsement, recommendation, or favoring by the United States Government or any agency thereof. The views and opinions of authors expressed herein do not necessarily state or reflect those of the United States Government or any agency thereof.

Kipp fragmentation theory<sup>2</sup>. These simulations strongly suggest that determination of the thermal damage states, prior to the onset of ignition, are key to assessing the degree of reaction violence.

## DESCRIPTION OF THE CONTINUUM MIXTURE MODELING

Accelerated combustion, following thermal ignition, is modeled using a description that has been implemented in shock physics analysis. Foundation for this approach is based on the continuum theory of multiphase reactive mixtures by Baer and Nunziato<sup>10</sup>. For the sake of brevity, only the final forms of this model are given here. This model has been shown to describe deflagration to detonation states in porous energetic materials. Furthermore, its implementation into the shock physics code, CTH<sup>11</sup>, provides a means for assessing the effects of fast combustion and the response of confinement.

In this approach, a continuum average is imposed over each phase, and balance equations are formulated to treat a multi-component system. Associated with each phase, denoted with a subscript "a", are material partial densities,  $\rho_a = \phi_a \gamma_a$ , true material density,  $\gamma_a$ , volume fractions,  $\phi_a$ , particle velocities,  $\dot{v}_a$ , pressures,  $p_a$ , temperatures,  $T_a$ , and internal energies,  $e_a$ . The Eulerian forms of the balance laws are given as:

Mass:

$$\dot{\rho}_a = -\rho_a \nabla \cdot \dot{v}_a + c_a^\dagger \quad (1)$$

Momentum:

$$\rho_a \dot{v}_a = \nabla \cdot \sigma_a + \dot{m}_a^\dagger - c_a^\dagger \dot{v}_a \quad (2)$$

Energy:

$$\dot{\rho}_a e_a = \sigma_a \cdot \dot{v}_a + e_a^\dagger - (\dot{m}_a^\dagger - c_a^\dagger \dot{v}_a) \cdot \dot{v}_a - c_a^\dagger (e_a + (\dot{v}_a \cdot \dot{v}_a)/2) \quad (3)$$

where the material derivative for each phase is defined  $\dot{f} = \partial f / \partial t + \dot{v}_a \cdot \nabla f$ . The "†" superscript denotes a phase exchange quantity for mass,  $c_a^\dagger$ , momentum,  $\dot{m}_a^\dagger$ , and energy,  $e_a^\dagger$  and the stresses are represented as  $\sigma_a = -\phi_a p_a I + \tau_a$ .

Consistent with derivations used in mixture theory, summation of each balance equation over all phases yields the response of the total mixture corresponding to the well known equations of motion for a single phase material. Thus, summation constraints are imposed on the phase interactions:  $\sum c_a^\dagger = 0$ ,  $\sum \dot{m}_a^\dagger = 0$  and  $\sum e_a^\dagger = 0$ . The restrictions of the Second Law of Thermodynamics also suggest admissible forms of phase interaction. The algebraic manipulations are not given here and the final forms of these interactions are as follows:

$$\dot{m}_a^\dagger - c_a^\dagger (\dot{v}_a + \dot{v}_i)/2 + p_i \nabla \phi_a = \sum_j \delta_{j,a} (\dot{v}_j - \dot{v}_a) \quad (4)$$

$$e_a^\dagger - \dot{m}_a^\dagger \cdot \dot{v}_a - (e_a - \dot{v}_a \cdot \dot{v}_a/2) c_a^\dagger - (\beta_a - p_a) (\phi_a - c_a^\dagger / \gamma_a) = \sum_j \mathcal{H}_{j,a} (T_j - T_a) \quad (5)$$

$$\phi_a - c_a^\dagger / \gamma_a = \sum_j \tau_{j,a} (p_a - \beta_a - p_j + \beta_j) \quad (6)$$

where  $\delta_{j,a}$ ,  $\mathcal{H}_{j,a}$ ,  $\tau_{j,a}$  are exchange coefficients of positive-definite symmetric tensors reflecting interactions between phases. Interface quantities are denoted with a subscript "i". The configurational stress,  $\beta_a$ , is the stress associated with contact forces between phases and is a different stress state than the bulk stress associated with the material compressibility. Model closure is obtained by specifying an independent equation of state for each phase. Hence, the mixture description centers on the determination of appropriate constitutive relations and phase exchange coefficients using micromechanical modeling and/or experimental guidance.

Having established the general equations of motion for a multiphase mixture, the conservation equations are recast into an integral form consistent with the shock physics modeling of CTH<sup>12</sup>. Overall conservation of mass, momentum and energy is preserved and relative flow effects arise as phase diffusion effects due to velocity differences between individual phase particle velocities and the mixture mass-averaged velocity, i.e.  $\dot{v}_a = \dot{v}_a - \dot{v}$ . Phase interaction effects, such as mass exchange, drag and heat transfer, appear as cell volume-averaged quantities. A detailed derivation of the set of integral equations is given in Reference 13.

The phase conservation equations, in finite volume form, have a common mathematical structure:

$$\frac{d}{dt} \int_{\beta} f_a dV = \int_{\beta} R_a dV - \oint_{\partial\beta} (F_a \cdot \hat{n}) dS - \oint_{\partial\beta} f_a (u_a \cdot \hat{n}) dS \quad (7)$$

All of the multiphase conservation equations have source and phase diffusion terms. The cell-surface forces and phase diffusion effects (the two surface integrals in Equation 7, respectively) are incorporated in a step using operator splitting whereby all phase quantities are transported in or out of cells. The remaining cell volume source quantities,  $R_a$ , are resolved during a Lagrangian step. Details of numerical implementation into the shock physics code CTH are given in Reference 11.

### VARIABLE CONFINEMENT COOKOFF TEST (VCCT)

As a representative cookoff experiment, the VCCT geometry is modeled to illustrate the various modes of combustion and level of violence predicted by a CTH model for slow cookoff accident scenarios. The response is calculated for varied states of thermal damage by specifying porosity and specific surface area of the energetic material. A schematic diagram of the VCCT geometry is shown in Fig. 1. The test consists of a cylindrical geometry which confines the energetic material with an aluminum sleeve and a variable thickness steel sleeve<sup>14</sup>. Steel witness plates at either end provide axial confinement and washers are used to center the energetic material between the plates. The heating for the cookoff test is done by heater bands located on the outside of the steel confinement sleeve. In a typical VCCT slow cookoff test the temperature is quickly ramped to 100 C in one hour and then the confinement is thermally-soaked for two hours at temperature. At slow cookoff conditions, heating occurs at a rate of 3.3 C/hr until ignition. Figure 2 displays heat transfer analysis for the VCCT test with confined HMX. At these heating conditions, thermal ignition is predicted to occur when the temperature at the aluminum sleeve reaches ~190 C and the location of thermal runaway takes place at the center of the HMX at a time of 30 hours 27 minutes.

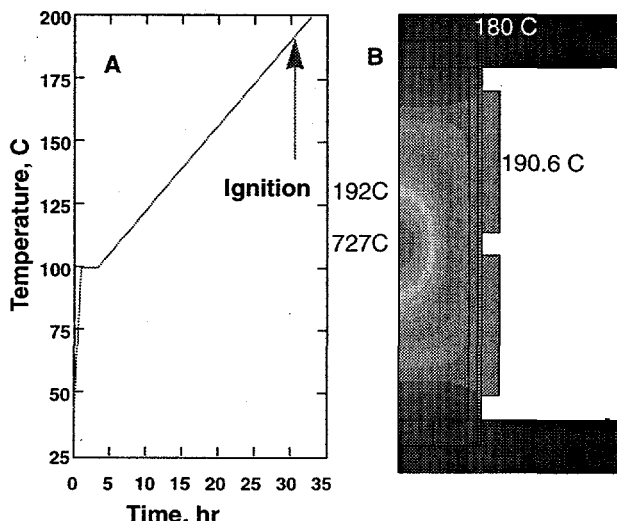


Fig. 2. A) Temperature boundary condition for cookoff analysis B) Predicted temperature profile illustrating the local ignition point in the energetic material.

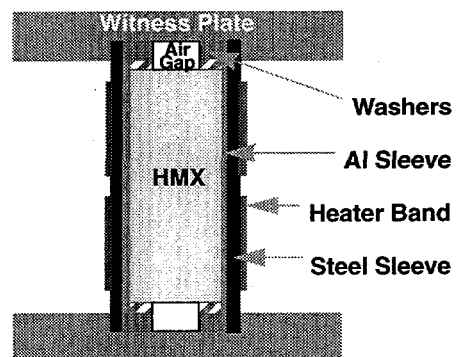


Fig. 1. Variable confinement cookoff test geometry.

At slow cookoff conditions, heating occurs at a rate of 3.3 C/hr until ignition. Figure 2 displays heat transfer analysis for the VCCT test with confined HMX. At these heating conditions, thermal ignition is predicted to occur when the temperature at the aluminum sleeve reaches ~190 C and the location of thermal runaway takes place at the center of the HMX at a time of 30 hours 27 minutes.

The calculated time to ignition is in agreement with the experimental data<sup>15</sup>. Figure 2.B displays the temperature field predicted using the COYOTE finite element code<sup>8</sup> at a time near the onset to self-sustained reaction. High temperatures develop at the center of the energetic material as a consequence of reaction in the HMX. The surrounding HMX is at much lower temperatures of the order 180 - 192 C due to heat loss to the confinement.

### DYNAMIC ANALYSIS OF COOKOFF

In modeling the VCCT experiment and assessing the violence of reaction during cookoff, it is necessary to define appropriate inputs for thermal damage states evolving prior to thermal runaway. Although much work has focused on determining stress-strain and decomposition rate data, relatively little experimental and modeling work has yet been done in characterizing the physical state of thermally-degraded energetic materials. Existing constitutive models, such as the reactive elastic-plastic

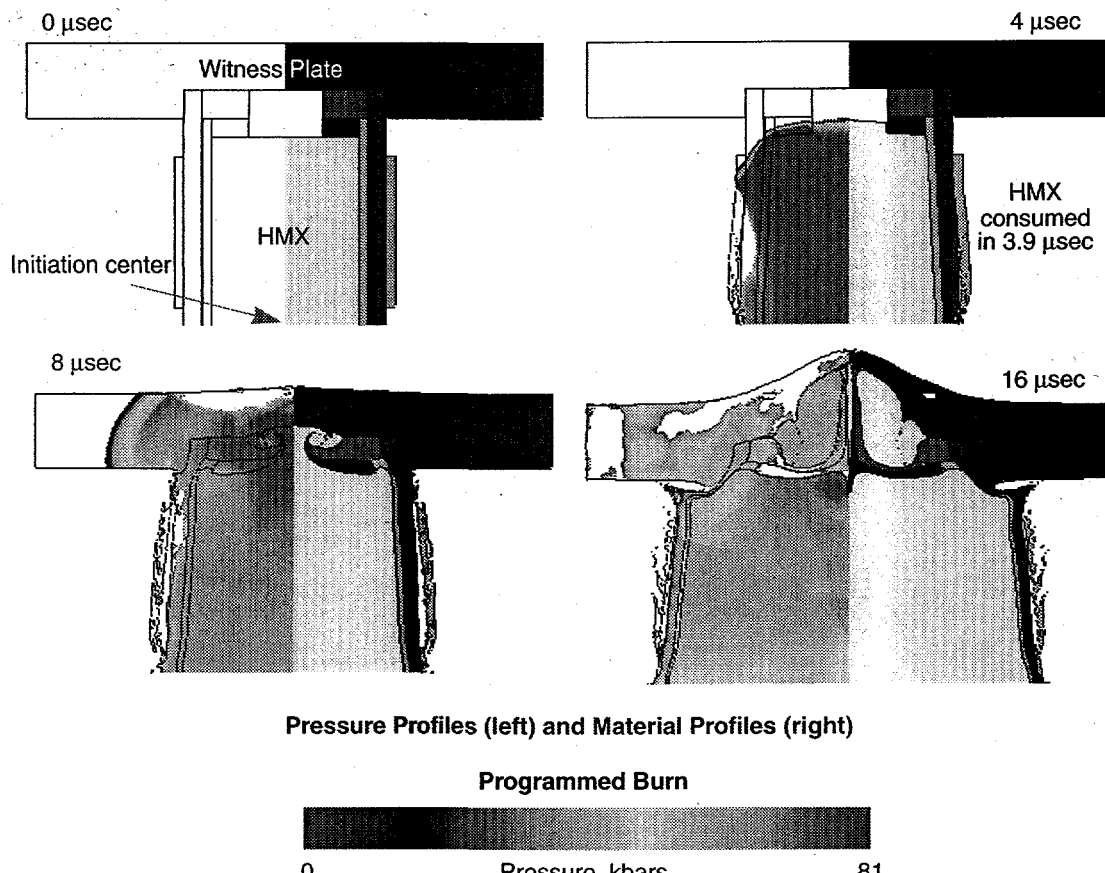


Fig. 3. Temporal response of VCCT confinement containing undamaged HMX during a detonation cookoff event.

(REP) model<sup>16</sup>, define hydrostatic stress for evolving decomposition. This model has been marginally successful in describing the response of confined energetic materials in "hot-cell" experiments<sup>17</sup>. The effects of phase change and relaxation phenomena, seen in experimental measurements, are not currently included in this model. Unfortunately, "fine tuning" this stress-strain relationship falls short of defining thermal damage states. Models for nucleation and coalescence must also be included in these descriptions. There does not currently exist any experimental guidance for developing predictive models of thermal damage states. Furthermore, the combustion behavior and shock sensitivity of thermally-degraded material are not well understood<sup>18</sup>.

In light of much uncertainty in the behavior of thermally degraded energetic materials, the approach used here is to specify the porosity and specific surface area for thermally damaged material. In these studies, HMX is the energetic material and burn rate and shock sensitivity are assumed to be similar to those for undamaged material<sup>19,20</sup>. Additionally, confinement is treated using elastic-perfectly plastic materials. In all of these numerical experiments, combustion is initiated at the center location of the confinement corresponding to the slow-cookoff heating conditions of the previous section. A point source of high pressure hot gas is imposed at the center ignition location to trigger the dynamic event. The pressure is assumed to be representative of a constant volume explosion state<sup>21</sup>.

In these numerical simulations, the VCCT geometry is assumed to be radially and axially symmetric, thus a quarter of the geometry is modeled. To resolve the mechanical response of confinement, a minimum of ten cells in the thinnest layer of the confinement is required. Thus, the computational domain represents  $300 \times 300$  cells. Analysis of results are displayed at selected time planes in which materials (right) are mirrored to pressure contour fields (left).

Case 1: As a baseline case, a numerical simulation has first been provided which considers a point initiated detonation as shown in Figure 3. A program-burn detonation model is used in this simulation. A spherically expanding wave spreads through undamaged HMX (100% TMD) and interacts with the cylindrical confinement. The detonation wave consumes all of the HMX in  $\sim 3.9 \mu\text{s}$ . At  $8 \mu\text{s}$ , the apparatus undergoes large deformation, and breakup of the confinement begins. At  $16 \mu\text{s}$  the confinement has failed and the witness plates are breached. This case represents the most violent cookoff response since it corresponds to the highest energy release in the shortest amount of time.

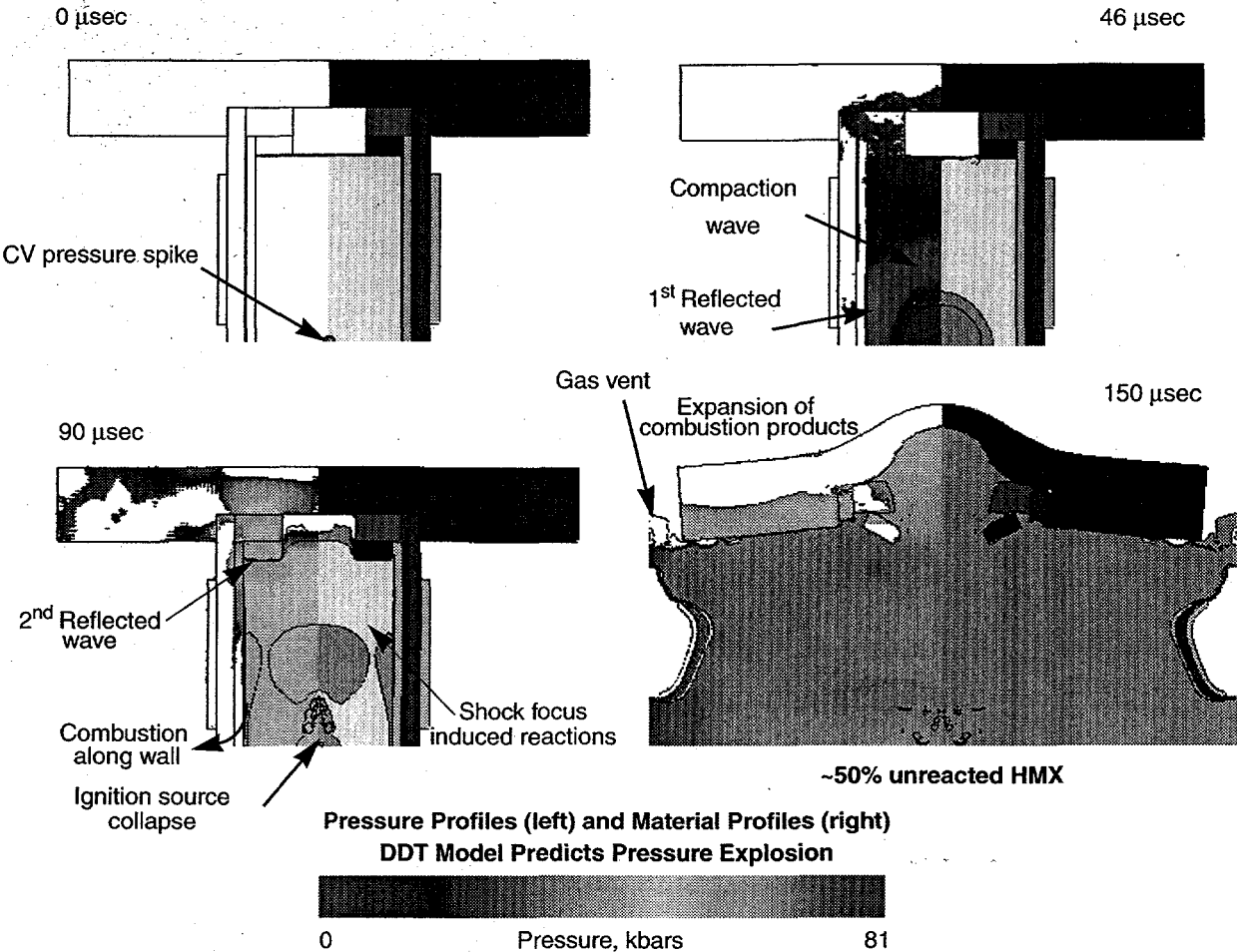


Fig. 4. Temporal response of VCCT geometry during a high-speed deflagration cookoff event in damaged HMX at 35% porosity and specific surface area of  $250 \text{ cm}^{-1}$ .

Many experimental studies<sup>22,23,24</sup> suggest that the energy release is much lower than that which results from detonation. Cookoff responses are more likely to be due to a very fast burn that can rapidly accelerate and, given enough distance, create pressure waves which coalesce into a combustion-supported shock wave. An appropriate approach to investigate this combustion behavior is a model for reactive multiphase mixtures, discussed in the previous section, as implemented in the shock physics code, CTH. This model predicts self-accelerated combustion and the resulting depressurization and extinguishment due to loss of confinement.

Case 2: Figure 4 shows a set of time-planes for a VCCT cookoff experiment in which a high-speed deflagration occurs in thermally damaged HMX. This corresponds to a condition where the HMX has decomposed prior to thermal runaway to a uniform state having 35% porosity and a specific surface area of  $250 \text{ cm}^{-1}$ . After ignition, the pressure pulse initiates a deflagration associated with compression of the compaction wave. At  $\sim 40 \mu\text{s}$ , the compaction wave reaches the confinement walls and stagnation of material causes pressure rise that strengthens subsequent reactions. This amplified wave initiates combustion along the wall and at  $\sim 90 \mu\text{s}$  compaction reflects off the witness plate. Material then expands across the washer gap and the entire energetic material is pressurized and undergoes volumetric burning. This rapid combustion leads to failure and fragmentation of the apparatus. In contrast to the detonation calculation, the events occur on a time scale that is an order of magnitude longer than that of detonation. At the time when the confinement begins to fail, venting of the combustion product gases causes a rapid pressure drop which quenches the reaction. Approximately 50% of the HMX has been consumed during this type of cookoff event, indicating a much lower energy release than that of detonation.

Case 3: In the next numerical simulation, self-accelerated combustion takes place in 85% TMD HMX (15% porosity) having a specific surface area of  $\sim 50 \text{ cm}^{-1}$ . This represents a reduced state of thermal damage as compared to case 2. Although more energetic mass potentially participates in the combustion event, lower specific surface area

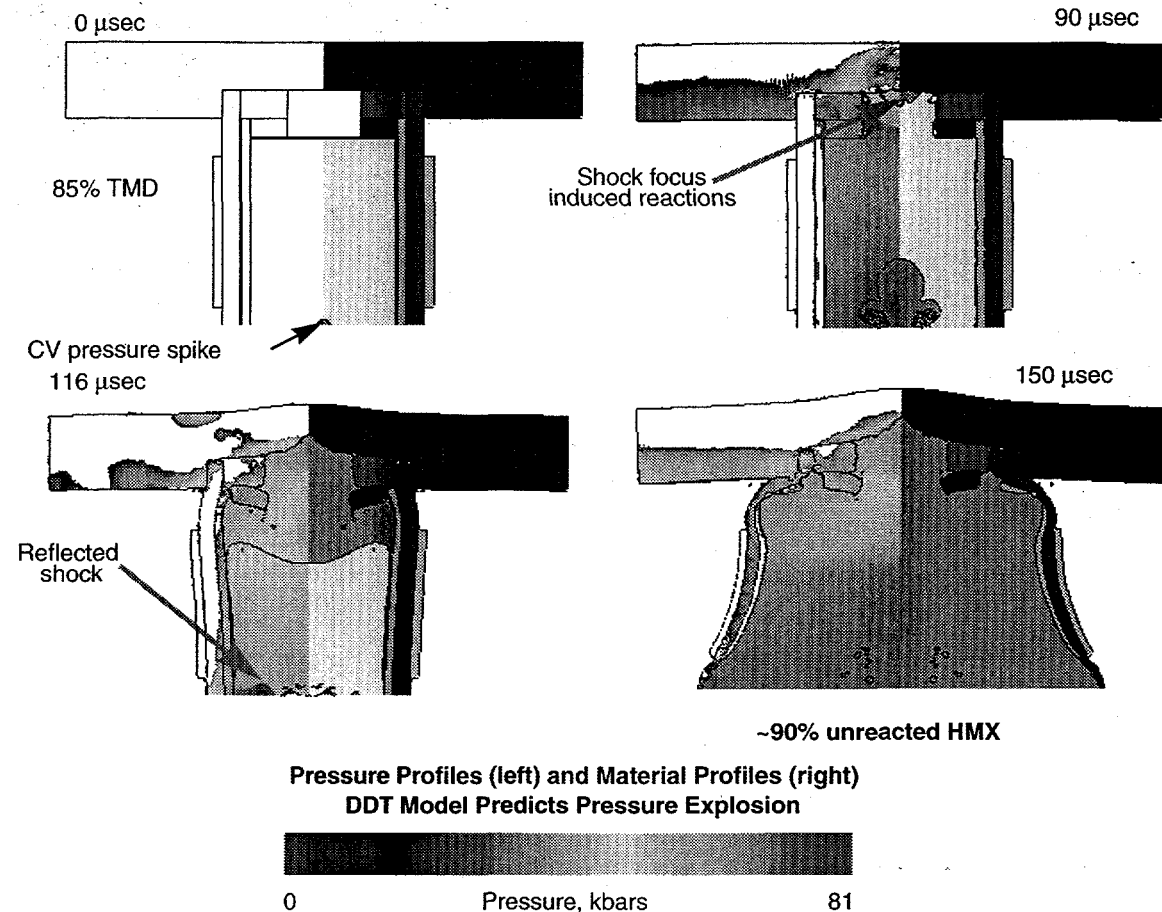


Fig. 5. Temporal response of VCCT experiment in which accelerated combustion occurs in HMX with reduced thermal damage having 15% porosity and specific surface area of  $50 \text{ cm}^{-1}$ .

implies a reduced the rate of energy release. Thus, a different sequence of combustion processes takes place whereby reduced pressure buildup interacts with the confinement (as seen in Fig. 5).

In this case, the compaction wave induced by the ignition pulse is weak and when it interacts with the walls of confinement slow reaction continues to occur in contrast to the enhanced grain burning seen in Case 2. This reactive compaction wave passes through the energetic material and after interacting with the witness plate, it strengthens and traverses back into reacting material. Similar to the prior case, all of the energetic material undergoes pressure-dependent combustion. The confinement breaks apart before a large fraction of the energetic material is consumed at high pressure. After  $\sim 150 \mu\text{s}$ , the confinement has ruptured and pressure release quenches the combustion. In this case, roughly 10% of the HMX mass has participated in the cookoff event.

**Case 4:** In the last numerical simulation, the effect of thermal and mechanical loading during preheat is examined for HMX at a density of 65% TMD (35% porosity) having a specific surface area of  $\sim 250 \text{ cm}^{-1}$ . Using the calculated thermal field given in Figure 2, quasi-static stresses are estimated using finite element mechanics analysis, TREX3D<sup>25</sup>. Near ignition, the HMX is estimated to be stressed to  $\sim 2 \text{ kbar}$  due to the effects of thermal stress and gas pressurization. The stress and temperature fields determined by finite element analysis is then mapped to CTH finite volume cells using the data translation software, MERLIN.<sup>26</sup>

Figure 6 displays four time planes of the cookoff event for these initial states. Since much of the HMX is pre-heated to temperatures near the onset of thermal runaway, the imposed gas pulse triggers an acoustic disturbance which quickly spreads across the damaged HMX. This wave triggers reaction and a nearly constant volume combustion event occurs. For this test case approximately 60% of the HMX is consumed in  $40 \mu\text{s}$ .

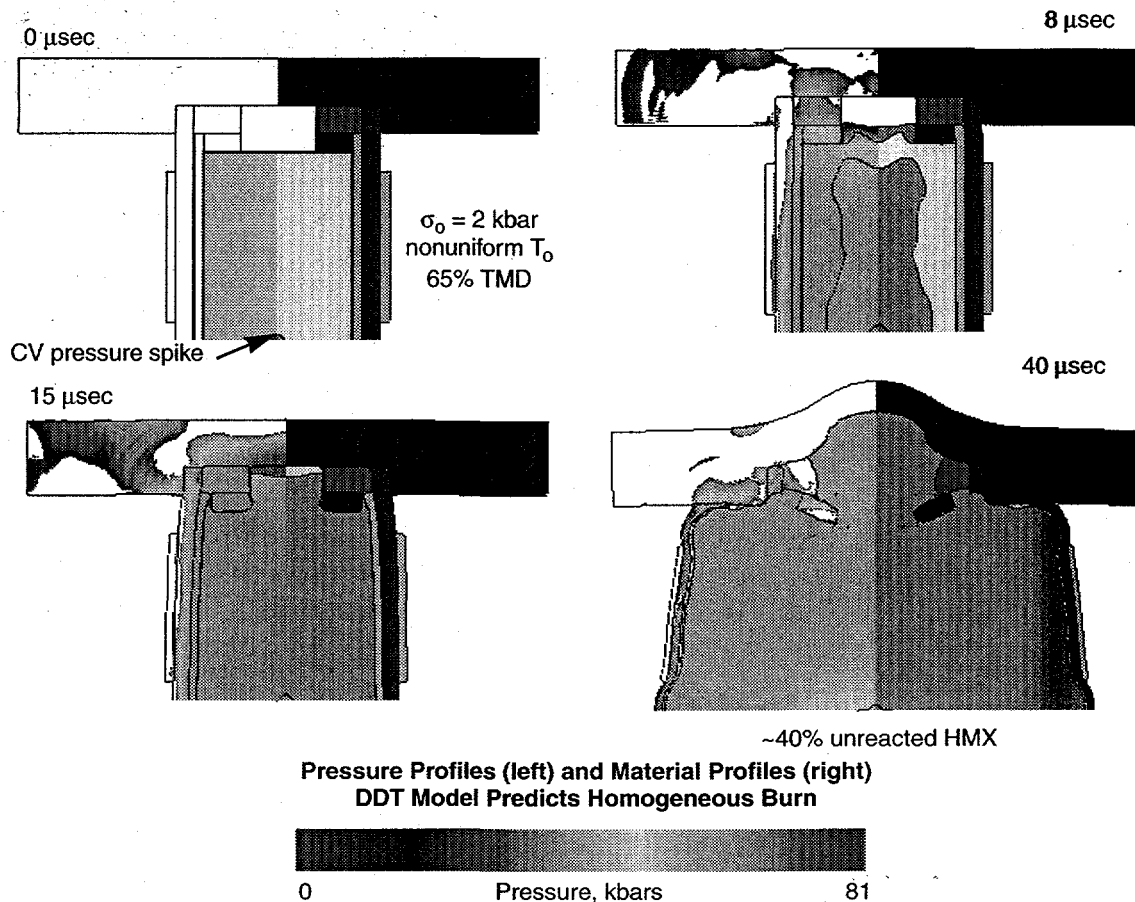


Fig. 6. Temporal response of the VCCT experiment confining thermally damaged HMX with 35% porosity and specific surface area of  $250 \text{ cm}^{-1}$  including the effects of thermal and pressure preloading prior to the onset of thermal runaway.

## CONFINEMENT FAILURE ANALYSIS

In a VCCT cookoff test, the level of violence is assessed by postmortem analysis of the test apparatus. A level of violence is based upon the number of fragments and the damage to the confinement. Accordingly, increasing violence events are classified as burn, pressure rupture, deflagration, explosion, partial detonation, and detonation. The distinctions between categories are very subjective.

Although the numerical simulations in the prior section indicate breakup of confinement, these material interfaces are a result of insertion of voids in computational cells when tension states exceeding a critical level. At best, these represent dynamic loading conditions near the onset of breakup of containment; a first principle resolution of breakup requires resolving to grain boundary length scales. As traditionally done in continuum modeling, one appeals to a damage model which describes fragmentation in terms of continuum variables. In this work, the fragmentation theory developed by Grady and Kipp<sup>2</sup> is used to estimate the approximate number and average size of fragments based upon a calculated strain rate. The average fragment size,  $s$ , is estimated using the formula,  $s = (\sqrt{24K/\rho c^3})^{2/3}$ , where  $K$  is the fracture toughness,  $\rho$  is the density,  $c$  is the speed of sound, and  $\dot{\epsilon}$  is the local strain rate.

Lagrangian tracers are used in the numerical simulations to monitor the hoop and axial stress states of the confinement. These strain rates are used with the Grady/Kipp correlation to bound average fragment sizes in the axial and circumferential direction. Thus, an average fragment geometry is estimated and the number of fragments is estimated by partitioning the confining shell into  $N$  average fragments.

To illustrate how this methodology is applied to cookoff simulations in which a violent detonation event occurs, the energy release rate is varied by modifying the wave speed to one half, and one eighth of the C-J detonation velocity.

ity for undamaged HMX. In all of these simulations, 100% of the energetic material is consumed during the cookoff event -- only the rate of energy release is modified. The calculated strain rates, average fragment size, and number of fragments for these conditions are shown in Table 1.

Table 1: Example Fragmentation Calculation

Energy Release Rate	$\dot{\epsilon}_{hoop}$ [1/s]	$s_{hoop}$ [mm]	$\dot{\epsilon}_{axial}$ [1/s]	$s_{axial}$ [mm]	Approximate Number of Fragments
$D_{cj}$	$5.5 \times 10^4$	3.4	$2 \times 10^4$	6.7	150
$1/2 D_{cj}$	$4.5 \times 10^4$	3.9	$5 \times 10^3$	17	100
$1/8 D_{cj}$	$1.4 \times 10^4$	10.6	$3 \times 10^3$	24	30

As one might expect, as the wave speed is reduced the rate of loading of the confinement decreases and larger fragments are predicted. Due to full energy release, a large number of fragments are expected. In the case of fast deflagration, the expected number of fragments are lower; however, there does not appear to be a well defined basis for defining a level of violence. Clearly, better diagnostics are needed to assess the level of violence in these cookoff tests. For example, the work of Ho<sup>23</sup> includes pressure gauges to monitor overpressure and impulse of the dynamic combustion events. Additional measurements of confinement strain and particle velocity would also yield more insight into the level of violence during cookoff.<sup>22</sup>

## SUMMARY AND CONCLUSIONS

In this work, a scoping analysis of the events following thermal runaway has been addressed. A key feature of cookoff response is the effect of thermal damage of the energetic material which evolves prior to ignition. Several numerical cases illustrate the effects of porosity and specific surface area which lead to different modes of self-accelerated combustion. Energetic materials with extensive thermal damage can potentially produce violent combustion events.

Much of this study illustrates that additional material characterization work needs to be investigated particularly as applied to the thermally-degraded energetic material. Modeling the level of violence requires better insights into the microstructure and morphological states of the damaged material. Furthermore, better combustion models require information on pressure dependent combustion rates and shock sensitivity of partially decomposed energetic materials.

As cookoff modeling matures, it will be necessary to also improve diagnostics to probe cookoff events. Current assessments such as those based on fragmentation characteristics are grossly inadequate. Instrumentation to probe the response of the confined energetic material, such as pressure or impulse and stress-strain states of confinement, may yield to better insights of cookoff behavior.

## ACKNOWLEDGEMENTS

This work was performed at Sandia National Laboratories supported by the U. S. Dept. of Energy under contract DE-AC04-94AL85000.

## REFERENCES

1. Alexander, K. and Gibson, K., "Variable Confinement Cookoff Test," Naval Surface Warfare Center, Indian Head Division, White Oak Detachment, Memorandum dated November 7, 1994
2. Kipp, M. E., Grady, D.E., and Swegle, J.W., "Numerical and Experimental Studies of High-Velocity Impact Fragmentation," Int. J. Impact Engng, Vol. 14, pp. 427-438 (1993)
3. Baer, M. R., Hobbs, M. L., Gross, R. J., Gartling, D. K., and Hogan, R. E., "Modeling Thermal/Chemical/Mechanical Response of Energetic Materials," PYROTECHNICS Basic Principles, Technology, Application, 26th International Annual Conference of ICT, Karlsruhe, Federal Republic of Germany, V37 (1995)

4. Renlund, A., Miller, J. C., Hobbs, M. L. and Baer, M. R., "Experimental and Analytical Characterization of Thermally Degraded Energetic Materials," JANNAF Propulsion Systems Hazards Subcommittee (PSHS) Meeting, Huntsville, Alabama (1995).
5. Behrens, R., Jr., "Thermal Decomposition of Energetic Materials: Temporal Behaviors of the Rates of Formation of the Gaseous Pyrolysis Products from Condensed-Phase Decomposition of Octahydro-1,3,5,7-tetranitro-1,3,5,7-tetrazocine," *J. Phys. Chem.*, **94**, 6706 (1990).
6. Renlund, A. M., J. C. Miller and K. L. Erickson, "Characterization of Energetic Material Response to Thermal Environments" 1996 JANNAF Propulsion Systems Hazards Subcommittee Meeting, Naval Postgraduate School, Monterey, CA (1996).
7. Nichols, A. L., Couch, R., Maltby, J.D., McCallen, R.C., Otero, I., and Sharp, R., "Couple Thermal/Chemical/Mechanical Modeling of Energetic Materials in ALE3D" 1996 JANNAF Propulsion Systems Hazards Subcommittee Meeting, Naval Postgraduate School, Monterey, CA (1996).
8. Gartling, D. K., and Hogan, R. E., "COYOTE II - A Finite Element Computer Program for Nonlinear Heat Conduction Problems," SAND94-1173, Sandia National Laboratories, Albuquerque, NM (1994).
9. Hobbs, M.L., Baer, M.R., and Gross, R.J., "Thermal, Chemical, and Mechanical Cookoff Modeling," JANNAF Propulsion Systems Hazards Subcommittee Meeting, San Diego, California (1994).
10. Baer, M.R., and Nunziato, J.W., "A Two-Phase Mixture Theory for Deflagration-to-Detonation Transition in Reactive Granular Materials," International Journal of Multiphase Flow, Vol. 12, pp. 861-889 (1986).
11. Baer, M. R., Hertel, E. S., and Bell, R.L., "Multidimensional DDT Modeling of Energetic Materials", 1995 APS Topical Conference on "Shock Compression of Condensed Matter" (1995).
12. McGlaun, J.M., Thompson, S.L., and Elrick, M.G., "CTH: A Three-Dimensional Shock Physics Code," *Int. J. Impact Engng*, Vol. 10, pp. 351-360 (1990).
13. Baer, M. R., "Continuum Mixture Modeling of Reactive Porous Media", Chapter 3, **High-Pressure Shock Compression of Solids, IV, Response of Highly Porous Solids to Shock Loading**, Series Editor R. A. Graham, Springer-Verlag (1996).
14. Peletski, C. and Gibson, K., "Variable Confinement Cookoff Test" 1996 JANNAF Propulsion Systems Hazards Subcommittee Meeting, Naval Postgraduate School, Monterey, CA (1996).
15. Gibson, K., "Variable Confinement Cookoff Test (VCCT) Results (Aug90-Nov91)," Memorandum dated December 6, 1991.
16. Hobbs, M.L., Baer, M.R., and Gross, R.J., "A Constitutive Mechanical Model for Energetic Materials," Twentieth International Pyrotechnics Seminar, Colorado Springs, Colorado, IIT Research Institute, Chicago, Illinois, (1994).
17. Hobbs, M. L., Schmitt, R. G., Renlund, A. M., "Analysis of Thermally-Degrading, Confined HMX," 1996 JANNAF Propulsion Systems Hazards Subcommittee Meeting, Naval Postgraduate School, Monterey, CA (1996).
18. Renlund, A. M, personal communication.
19. Boggs, T.L., "The Thermal Behavior of Cyclotrimethylenetrinitramine (RDX) and Cyclotetramethylenetrinitramine (HMX)," Chapter 2, Fundamentals of Solid Propellant Combustion, Progress in Astronautics and Aeronautics, (K.K. Kuo and M. Summerfield, Eds.), Vol. 90, pp. 121-175 (1984).
20. Sandusky, H. W. and Bernecker, R.R., "Compressive Reaction in Porous Beds of Energetic Materials," Eight Symposium (International) on Detonation, NSWC MP 86-194, pp 881-891 (1985).
21. Fried, L. E., "CHEETAH 1.39 User's Manual", UCRL-MA-1175, Lawrence Livermore National Labs (1996).
22. Chidester, S.K., Tarver, C.M., Green, L.G, and Urtiew, P.A., "On the Violence of Thermal Explosion in HMX- and TATB Solid Explosives," submitted to *Combustion and Flame* (1996).
23. Ho, S.Y., "Thermomechanical Properties of Rocket Propellants and Correlation with Cookoff Behavior," *Propellants, Explosives, Pyrotechnics*, Vol. 20, pp. 206-214 (1995).
24. Scholtes, J.H.G., NIMIC/TCCP Cookoff Workshop, NAWC Conference Center, March 12-13 (1996)
25. Gross, R.J., "A Direct Fortran Coupling of COYOTEII and JAS3D to Perform Thermal/Chemical/Mechanical Analyses," Sandia National Laboratories Memorandum dated December 13, 1995
26. Gartling, D.K. "MERLIN II - A Computer Program to Transfer Solution Data between Finite Element Meshes," SAND89-2989, Sandia National Laboratories, Albuquerque, NM, (1991).